Interband polarization spectroscopy to test the spherical model of a shallow acceptor in δ-doped heterostructures

2007 J. Phys.: Condens. Matter 19 236205

(http://iopscience.iop.org/0953-8984/19/23/236205)

IOP PUBLISHING JOURNAL OF PHYSICS: CONDENSED MATTER

J. Phys.: Condens. Matter **19** (2007) 236205 (11pp) doi:10.1088/0953-8984/19/23/236205

Interband polarization spectroscopy to test the spherical model of a shallow acceptor in δ-doped heterostructures

J Łusakowski[1], R Buczko[2], M Sakowicz[1], K J Friedland[3], R Hey[3] and K Ploog[3]

[1] Institute of Experimental Physics, University of Warsaw, Hoża 69, 00-681 Warsaw, Poland
[2] Institute of Physics, Polish Academy of Sciences, Aleja Lotników 32/46, 02-668 Warsaw, Poland
[3] Paul-Drude-Institut für Festkörperelektronik, Hausvogteiplatz 5-7, 10117 Berlin, Germany

E-mail: jerzy.lusakowski@fuw.edu.pl

Received 25 January 2007, in final form 13 April 2007
Published 8 May 2007
Online at stacks.iop.org/JPhysCM/19/236205

Abstract

Photoluminescence measurements were carried out on Be δ-doped GaAs/$Al_{0.33}Ga_{0.67}As$ heterostructure at 1.6 K in magnetic fields (B) up to 4 T. Luminescence originating from recombination of a two-dimensional electron gas (2DEG) and photoexcited holes localized on Be acceptors was analysed. The degree of circular polarization (γ_C) of the luminescence from fully occupied Landau levels was determined as a function of B and the 2DEG concentration, n_s. At constant B, γ_C decreased with the increase of n_s. The intensity of the optical transition considered was calculated, taking into account the s-like and d-like parts of the acceptor envelope function. It is shown that the presence of the d-like part explains the observed $\gamma_C(n_s)$ dependence quantitatively. Two other possible mechanisms of the $\gamma_C(n_s)$ dependence were excluded: the Stark effect on a hole bound to a Be acceptor and the Pockels effect, i.e. the in-plane anisotropy induced by the heterostructure electric field. Thus, it is shown that polarization spectroscopy on acceptor δ-doped heterostructures enables one to test experimentally the contribution of the $L > 0$ component of the envelope in a shallow acceptor description.

1. Introduction

In acceptor δ-doped GaAs/AlGaAs heterostructures, a diluted sheet of acceptors is introduced some tens of nanometres from the GaAs/AlGaAs interface, and a two-dimensional electron gas (2DEG) is created due to doping of a barrier with shallow donors. A photoluminescence experiment on such structures reveals (among other features) a spectrum corresponding to the recombination of 2D electrons with holes localized in the δ-layer. An analysis of the degree of

circular polarization (γ_C) of this transition as a function of the magnetic field (B) allows one to investigate the spin polarization of a 2DEG in the regime of the integer and fractional quantum Hall effects [1]. An interpretation of experiments presented in [1] was based on a model in which the ground state of a shallow acceptor in GaAs was described by an s-like envelope function (the '$L = 0$ model'). According to this model, γ_C depends *only* on the magnetic field and the temperature (T): the magnetic field splits the electron and hole levels, which are populated according to a thermal distribution at given T. Within this approach, the properties of a 2DEG could have been analysed because the properties of holes localized on acceptors were assumed to be known.

According to our experimental studies, γ_C also depends on the concentration of the 2DEG (n_s) when B and T are constant. To explain the effect observed, we analyse three mechanisms: the Stark effect on a photoexcited hole bound to a Be acceptor (mixing of hole levels by the heterostructure electric field), the Pockels effect (in-plane anisotropy of optical transitions induced by the heterostructure electric field), and an influence of a d-like part of the acceptor envelope on γ_C. We show that the Stark and Pockels effects are negligible in the heterostructure investigated, and it is the presence of a d-like part of the envelope that is responsible for the $\gamma_C(n_s)$ dependence observed.

The paper is organized as follows. Sections 2 and 3 describe the experimental procedure and results. Section 4 contains a theoretical analysis of the intensity of the optical transition considered, the results of calculations and their comparison with experimental data. It is shown that γ_C calculated within the spherical model which takes into account both s-like and d-like parts of an acceptor envelope (the '$L = 0, 2$ model'), describes the experimental $\gamma_C(n_s)$ dependence quantitatively. In section 5, we estimate changes in γ_C resulting from the Stark and Pockels effects. Finally, we summarize and conclude the paper.

2. Experiment

The sample under investigation was a high-quality GaAs/$Al_{0.33}Ga_{0.67}As$ heterostructure grown on semi-insulating GaAs substrate. The GaAs channel of about 1 μm above 50 periods of 5 nm/5 nm GaAs/AlAs superlattice contains unintentional acceptors at a concentration less than 10^{14} cm^{-3}. The AlGaAs barrier comprises an undoped 45 nm thick AlGaAs spacer and a uniformly Si-doped 35 nm thick AlGaAs layer; the doping level amounts to 10^{18} cm^{-3}. The δ-layer of Be atoms with the concentration of 10^9 cm^{-2} was introduced into the GaAs channel at the distance $z_0 = 30$ nm away from the GaAs/AlGaAs interface. The barrier was covered with a 15 nm thick GaAs cap layer.

The measurements were carried out in an optical helium cryostat supplied with a split coil. All measurements were carried out at 1.6 K, and the temperature was stabilized within 0.02 K by pumping the helium gas through a manostat. The luminescence was excited by a He–Ne laser. All data presented in this paper were obtained at the same laser excitation power. The power of excitation was a few mW cm^{-2}, and was a few orders of magnitude smaller than that corresponding to a saturation of the luminescence signal. Both continuous-wave (cw) and time-resolved measurements were performed. In the latter case, laser pulses were generated by passing the laser beam through an acoustooptical modulator driven by a generator of rectangular voltage pulses. The time resolution was 5 ns. The luminescence passed through a $\lambda/4$ plate followed by a quartz linear polarizer. The circular polarizations were separated by turning the $\lambda/4$ plate. The luminescence was analysed by a spectrometer supplied with a charge-coupled device (CCD) camera (for cw measurements) or with a photomultiplier (for time-resolved measurements). In the latter case, the photomultiplier signal was directed to a photon counter.

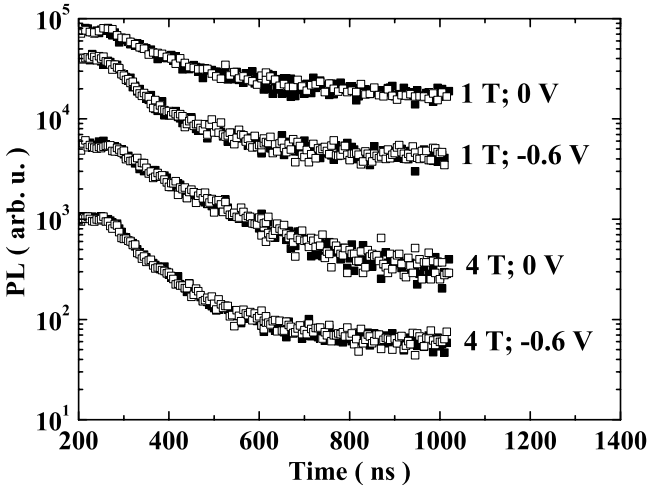

Figure 1. Examples of the time dependence of the σ^- (solid squares) and σ^+ (open squares) components of the luminescence from $N = 0$ LLs for two values of B and applied gate polarizations (indicated). Each σ^- signal was scaled to coincide with the corresponding σ^+ signal. The exciting laser pulse ends at about 270 ns.

A semi-transparent Au gate electrode and an ohmic contact were fabricated on the sample surface, and the concentration of the 2DEG was tuned by polarizing the gate in the backward direction. n_s was estimated by determination of the magnetic field, $B_{\nu=2}$, at which the luminescence from the $N = 1$ Landau levels (LLs) disappears (two Landau levels correspond to each N). Then $n_s = 2B_{\nu=2}/(h/e)$, where e is the electron charge and h is the Planck constant.

3. Results

Figure 1 shows examples of the temporal evolution of the luminescence signals measured in σ^+ (open squares) and σ^- (solid squares) circular polarizations. The σ^- data were multiplied by a constant factor to coincide with the σ^+ data. Corresponding σ^+ and σ^- signals are proportional one to each other over the whole time domain, both within the laser pulse, and after the pulse end. This means that the degree of polarization does not depend on time (within the time resolution of the present experiment), which indicates that the system is stationary and time-resolved polarization measurements give the same value of γ_C as cw measurements. We used this fact to analyse polarization data obtained from cw measurements, which essentially improved the signal to noise ratio. The fact that the system investigated is stationary does not necessarily mean that the distribution of holes on acceptor levels corresponds to the temperature of the helium bath surrounding the sample. We refer here to time-resolved polarization studies on similar structures [2] which show that at 1.6 K the relaxation time of photoexcited holes on the acceptor levels is of the order of 10^{-10}–10^{-9} s. This is a few orders of magnitude shorter than the luminescence decay time, which is of the order of 10^{-7} s, as can be deduced from figure 1. For this reason, we can assume that photoexcited holes are distributed on the acceptor levels according to an equilibrium thermal distribution corresponding to the helium bath temperature of 1.6 K.

The problem of distribution of electrons is avoided in the present considerations because we take into account the luminescence originating from fully occupied Landau levels only.

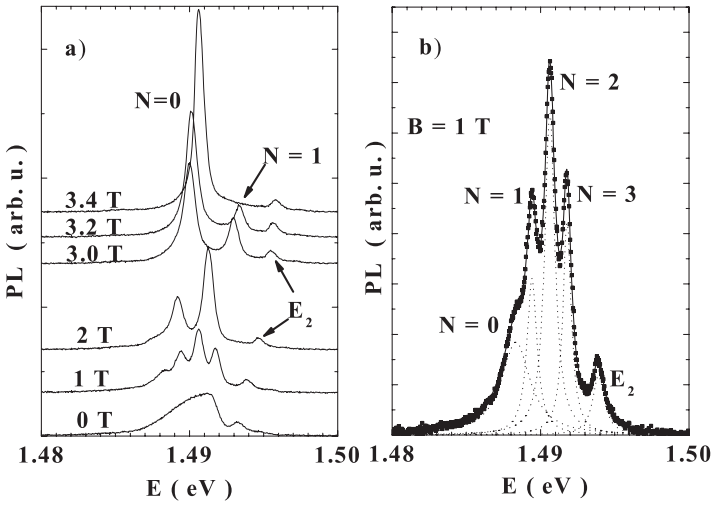

Figure 2. (a) Evolution of the luminescence spectrum with the magnetic field B (indicated). LLs of the ground electrical subband and the peak corresponding to the first excited (E_2) subband are visible. The LLs are labelled with their number, N. In this case, the $N = 1$ peak disappears at $B_{\nu=2} \approx 3.3$ T. The spectra are vertically shifted for better presentation. (b) An example of deconvolution of a luminescence spectrum into Lorentzians.

An example of the magnetic field evolution of the luminescence spectrum is shown in figure 2(a). With an increase of B, the number of populated LLs of the first electrical subband decreases as their degeneracy grows. The analysis of the polarization of the luminescence starts with a deconvolution of each spectrum into separate Lorentzian peaks corresponding to pairs of LLs (figure 2(b)). We subtract from the total spectrum Lorentzians corresponding to the second electrical subband and the highest in energy pair of LLs of the first electrical subband (E_2 and $N = 3$ peaks in figure 2(b)). This leaves that part of the spectrum which corresponds to an equal number of LLs occupied with spin-up and spin-down electrons, i.e., to a totally unpolarized electron gas. The area of that part of the spectrum (I_{σ^+} or I_{σ^-} for σ^+ and σ^- polarization, respectively) is used to calculate $\gamma_C = (I_{\sigma^-} - I_{\sigma^+})/(I_{\sigma^-} + I_{\sigma^+})$. This procedure allows one to determine γ_C at given B for different n_s. The results are shown in figure 3(a). Clearly, γ_C depends on n_s, and to interpret this result is the purpose of the present paper.

4. Polarization of the $\Gamma_6 \rightarrow \Gamma_8$ transition within the spherical model of an acceptor ground state

The interpretation of the $\gamma_C(n_s)$ dependence observed is based on calculations of matrix elements of the optical transition considered within the following model. The ground state of the system is represented by an ionized shallow acceptor located at $z_0 = 30$ nm from the heterostructure interface. The excited state is given by an electron which is created in one of Landau levels and a hole in the shallow acceptor ground state. We use an approximate description of the excited state neglecting the Coulomb interaction between the electron and the neutral acceptor, i.e., we neglect the excitonic effect for the exciton bound to an ionized acceptor. An experimental argument supporting this approximation is a linear (not quadratic) dependence of the luminescence energy on the magnetic field.

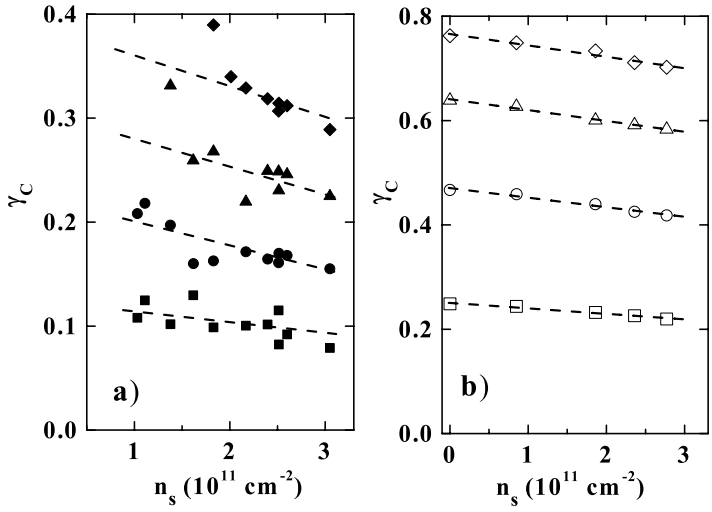

Figure 3. (a) Measured $\gamma_C(n_s)$ dependence for 1 T (squares), 2 T (circles), 3 T (triangles) and 4 T (diamonds). Dashed lines are (shifted) results of model calculations. (b) Model calculations of $\gamma_C(n_s)$ within the $L = 0, 2$ model for 1 T (squares), 2 T (circles), 3 T (triangles) and 4 T (diamonds). Dashed lines are linear fits. Points for $n_s = 0$ result from the $L = 0$ model.

We apply the dipole approximation for optical transitions and the one-electron description of electronic bands. Then, a matrix element of the transition is proportional to $\langle\psi_i|\hat{p}_{1,\pm1}|\chi_j\rangle$, where $|\psi_i\rangle$ and $|\chi_j\rangle$ are the one-electron Landau and acceptor states, respectively, and subscripts i and j represent appropriate sets of quantum numbers. The electronic $\chi_j(\mathbf{r})$ wavefunction is obtained by the time reversal of the bound hole wavefunction. The component $+1(-1)$ of the momentum operator ($\hat{p}_{1,\pm1} = \mp(\hat{p}_x \pm \mathrm{i}\hat{p}_y)$) is used according to the circular polarization σ^+ (σ^-) of the emitted photon.

In our calculations, the effective mass approximation has been used for the description of electronic wavefunctions. We also assume that the electron effective mass in the 2D conduction subband is isotropic and we use the spherical approximation of the shallow acceptor in the bulk GaAs, as described in the paper by Baldereschi and Lipari [3]. With all the above approximations, we find that our system exhibits a cylindrical symmetry with respect to the axis perpendicular to the interface and passing through the acceptor location. In calculations, we choose this axis as the z-direction of the coordinate system. The projection of the angular momentum on this axis is a good quantum number, and it is equal to 0 for the ground state and ±1 for excited states of the system investigated.

The electron wavefunction in the nth electric subband has the form $\psi_i = \psi_n(z)\psi_{N,m}(\rho)\mathrm{e}^{\mathrm{i}m\phi}$, where $\rho = \sqrt{x^2 + y^2}$ and ϕ is the azimuthal angle in the xy-plane. The envelope $\psi_n(z)$ results from the self-consistent solution of the Schrödinger and Poisson equations. In these calculations, the overall charge neutrality was guaranteed by taking into account interface and surface charges, which also simulate the effect of the gate electrode and which are used to control the concentration of the 2DEG in the heterostructure. The results of the calculations are the subband energies and wavefunctions as a function of the total 2DEG concentration n_s. We note that, in our model, n_s influences γ_C via $\psi_n(z)$ functions only.

The functions $\psi_{N,m}(\rho)$ are analytical solutions of the Shrödinger equation in the symmetric gauge for the vector potential corresponding to the magnetic field $\vec{B}\|\hat{z}$. N is the Landau level number and $m\hbar$ is the zth component of the angular momentum ($m \leqslant N$).

Therefore, the wavefunction of an electron on a Landau level is given by

$$\psi_i(\mathbf{r}) = \psi_{n,N,m,j_z}(\mathbf{r}) = \psi_n(z)\psi_{N,m}(\rho)\mathrm{e}^{\mathrm{i}m\phi}u_{j=\frac{1}{2},j_z}(\mathbf{r}), \tag{1}$$

where $u_{j=\frac{1}{2},j_z} = |R_0, \frac{1}{2}, j = \frac{1}{2}, j_z\rangle$ is the Bloch wavefunction at the minimum of the conduction band in the bulk GaAs. It is an eigenfunction of the total angular momentum with $j = \frac{1}{2}$ and it is built with an s-type orbital R_0 and the spin $\frac{1}{2}$.

The ground state of a shallow acceptor is fourfold degenerate, and each of the four one-electron wavefunctions $\chi_j(\mathbf{r})$ can be obtained by the time reversal of the appropriate one-hole wavefunction. In the spherical approximation, the ground state is an eigenstate of the total angular momentum $F = \frac{3}{2}$ and [3]:

$$\chi_j = \chi_{\frac{3}{2},F_z} = |\tfrac{3}{2}, F_z\rangle = f_0|0, \tfrac{3}{2}, \tfrac{3}{2}, F_z\rangle + f_2|2, \tfrac{3}{2}, \tfrac{3}{2}, F_z\rangle, \tag{2}$$

where f_0 and f_2 are radial functions and $|L, J = \frac{3}{2}, F = \frac{3}{2}, F_z\rangle$ are built with spherical harmonics Y_{LM} and Bloch functions $u_{J=\frac{3}{2},J_z} = |R_1, \frac{1}{2}, J = \frac{3}{2}, J_z\rangle$. The latter functions are, in turn, built with sp^3 orbitals R_1 and the spin $\frac{1}{2}$. We choose the basis $u_{J=\frac{3}{2},\frac{3}{2}} = \frac{1}{\sqrt{2}}(X+\mathrm{i}Y)\alpha$, $u_{J=\frac{3}{2},\frac{1}{2}} = \frac{\mathrm{i}}{\sqrt{6}}((X+\mathrm{i}Y)\beta - 2Z\alpha)$, $u_{J=\frac{3}{2},-\frac{1}{2}} = \frac{\mathrm{i}}{\sqrt{6}}((X-\mathrm{i}Y)\alpha + 2Z\beta)$, $u_{J=\frac{3}{2},-\frac{3}{2}} = \frac{\mathrm{i}}{\sqrt{2}}(X-\mathrm{i}Y)\beta$, where X, Y and Z are functions transforming like x, y and z under operations of the $\mathrm{T_d}$ symmetry group, respectively [4].

The transition matrix elements are

$$\begin{aligned}\langle\psi_{n,N,m,j_z}|\hat{p}_{1,\pm1}|\chi_{\frac{3}{2},F_z}\rangle &= \sum_{L=0,2}\langle n, N, m, j_z|\hat{p}_{1,\pm1}f_{\mathrm{L}}|L, \tfrac{3}{2}, \tfrac{3}{2}, F_z\rangle \\ &= \sum_{L=0,2}\sum_{M=-L}^{L} C^{\frac{3}{2},F_z}_{L,M,\frac{3}{2},F_z-M}\langle R_0, \tfrac{1}{2}, \tfrac{1}{2}, j_z|\hat{p}_{1,\pm1}|R_1, \tfrac{1}{2}, \tfrac{3}{2}, F_z - M\rangle \\ &\quad\times\int\psi^*_n(z_0+z)\psi^*_{N,m}(\varrho)\mathrm{e}^{-\mathrm{i}m\varphi}f_{\mathrm{L}}(r)Y_{LM}(\vartheta,\varphi)\,\mathrm{d}^3r.\end{aligned} \tag{3}$$

C denotes Clebsch–Gordan coefficients resulting from a decomposition of $|L, J, F, F_z\rangle$ into products $|L, M\rangle u_{J=\frac{3}{2},J_z}$, $M = -L, \ldots, L$, and $Y_{LM}(\vartheta,\varphi) = \sqrt{\frac{(2L+1)(L-M)!}{4\pi(L+M)!}}P^M_{\mathrm{L}}(\cos\vartheta)\mathrm{e}^{\mathrm{i}M\varphi}$.

The matrix elements between Γ_6 and Γ_8 Bloch states in the bulk material are:

$$\langle R_0, \tfrac{1}{2}, \tfrac{1}{2}, j_z|\hat{p}_{1,\pm1}|R_1, \tfrac{1}{2}, \tfrac{3}{2}, J_z\rangle = -\sqrt{\tfrac{3}{2}}C^{\frac{1}{2},j_z}_{\frac{3}{2},J_z,1,\pm1}\begin{Bmatrix}1 & \frac{1}{2} & \frac{3}{2}\\ \frac{1}{2} & 1 & 0\end{Bmatrix}\langle R_0\|\hat{p}_1\|R_1\rangle = C^{\frac{1}{2},j_z}_{\frac{3}{2},J_z,1,\pm1}p$$

where p is a constant, the same for all matrix elements. Noticing that the integral in (3) is proportional to $\delta_{m,M}$, we finally find that

$$\langle\psi_{n,N,m,j_z}|\hat{p}_{1,\pm1}|\chi_{\frac{3}{2},F_z}\rangle = p\sum_{L=0,2}C^{\frac{3}{2},F_z}_{L,m,\frac{3}{2},F_z-m}C^{\frac{1}{2},j_z}_{\frac{3}{2},F_z-m,1,\pm1}\sqrt{\frac{(2L+1)(L-m)!}{4\pi(L+m)!}}\mathfrak{I}_{n,L,N,m}, \tag{4}$$

where $\mathfrak{I}_{n,L,N,m} = \int P^m_{\mathrm{L}}(\cos\vartheta)\psi^*_{N,m}(r\sin\vartheta)\psi^*_n(z_0 + r\cos\vartheta)f_{\mathrm{L}}(r)r^2\,\mathrm{d}r\,\mathrm{d}\cos\vartheta$.

The first form of the matrix element in equation (3) allows one to write down the general selection rule for the transition investigated: $m + j_z = F_z \pm 1$. Next, because $L = 0, 2$, $|m| \leqslant 2$. Additionally, $m \leqslant N$. The resulting selection rules are shown in figure 4(a) for the $L = 0$ model and in figure 4(b) for the $L = 0, 2$ model. In the case of the $L = 0$ model, the selection rules are independent of the Landau level number, N. For the $L = 0, 2$ case, this is true for $N \geqslant 2$ only. A different number of transitions for $N = 0, 1$ for σ^+ and σ^- results from the condition $m \leqslant N$.

The intensity observed in the $\sigma^\pm$ polarization is equal to

$$I_{\sigma^\pm} = \Xi\sum_{N,m,j_z}\sum_{F_z=\pm\frac{1}{2},\pm\frac{3}{2}} w_{N,m,j_z}w_i|\langle\psi_{n,N,m,j_z}|\hat{p}_{1,\pm1}|\chi_{\frac{3}{2},F_z}\rangle|^2, \tag{5}$$

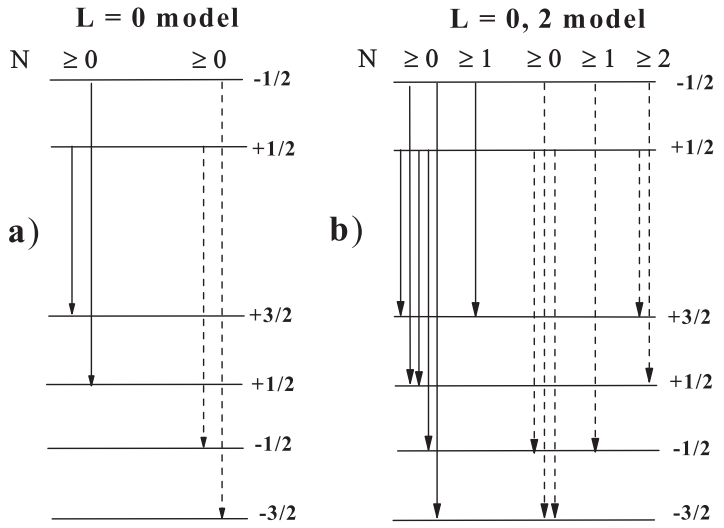

Figure 4. Selection rules for the $\Gamma_6 \rightarrow \Gamma_8$ transitions. Solid lines: σ^-, dashed lines: σ^+. Electron levels are described by $j_z = \pm 1/2$, and hole levels by $F_z = \pm 3/2, \pm 1/2$. Splitting of levels in a magnetic field is shown schematically only. (a) Selection rules for the $L = 0$ model of the acceptor envelope; (b) selection rules for the $L = 0, 2$ model of the envelope. N denotes the number of the Landau level and it is shown for what range of N a given transition is allowed.

where Ξ is a polarization-independent factor. Statistical weights w_i describe the probability of occupation of acceptor Zeeman levels: $w_i = \exp[(E_1 - E_i)/k_B T]/\sum_i \exp[(E_1 - E_i)/k_B T]$, where E_1 is the energy of the lowest-lying level. Statistical weights for electron levels, w_{N,m,j_z}, are equal to 1 because we consider only an equal number of fully occupied Landau levels with spin up and spin down. We used the above formulae to calculate γ_C for B from 1 to 4 T and for n_s from 0.86×10^{11} cm^{-2} to 2.77×10^{11} cm^{-2}, which corresponds to the ranges of B and n_s of interest.

Results of the calculations are shown in figure 3(b). If the $L = 2$ part of an acceptor envelope is neglected, then γ_C does not depend on n_s—the corresponding points are shown for $n_s = 0$. Taking into account the $L = 2$ part, one gets a decrease of γ_C with an increase of n_s.

There is an overall difference in measured and calculated γ_C values (compare figures 3(a) and (b)) which we attribute to a depolarization by the experimental system. What is essential for our considerations, however, is a dependence of γ_C on n_s for a constant B. Since the depolarization is constant at given B, we compare the measured results with the calculated results by shifting down the linear fits in figure 3(b) by an appropriate value to get fits that coincide with experimental data in figure 3(a). One can observe that variations of $\gamma_C(n_s)$ predicted by the $L = 0, 2$ model are in a quantitative agreement with measured dependences.

5. Discussion: the Stark and Pockels effects

Although the calculations presented in section 4 explain variations of the $\gamma_C(n_s)$ measured, we would like to show, before drawing the final conclusions, that other possible sources of the $\gamma_C(n_s)$ dependence can be neglected. We use in the following the $L = 0$ model, since we are interested now only in an estimation of the magnitude of possible effects. There are two factors that can contribute to a $\gamma_C(n_s)$ dependence: the heterostructure electric field and an internal stress. An internal stress, however, is practically absent in lattice-matched heterostructures,

and it can be neglected as well as stress-induced piezoelectric fields. The heterostructure electric field, E, causes two effects that can, in principle, lead to a $\gamma_C(n_s)$ dependence: the Stark effect and the Pockels effect. It will be shown below that both the effects double the number of allowed transitions shown in figure 4(a): each of transitions becomes active in both polarizations. This leads, in principle, to a decrease of γ_C as a function of E. In the following, the Stark and Pockels effects are discussed as a function of the electric field, E, but it is understood that E is coupled unequivocally to n_s. An appropriate relation can be established by self-consistent calculations of the heterostructure electrostatic potential, as was done in the present paper.

The Stark effect is a first-order perturbation on an acceptor bound hole. In the case of the electric field E and the magnetic field B in the z-direction, one has a perturbation Hamiltonian [5]:

$$H' = \mu_0(g_1' J_z + g_2' J_z^3)B + \frac{p}{\sqrt{3}}E(J_x J_y + J_y J_x), \tag{6}$$

where μ_0 is the Bohr magneton, g_1' and g_2' are isotropic and anisotropic g-factors, respectively, and p_d is the dipole moment of a Be acceptor.

Within the $L = 0$ model assumed in this section, the unperturbed acceptor wavefunctions are $f_0 u_{J=\frac{3}{2},J_z}$. In this basis, the Hamiltonian (6) takes the form

$$H' = \begin{bmatrix} b_1 & 0 & \mathrm{i}\epsilon_L & 0 \\ 0 & b_2 & 0 & \mathrm{i}\epsilon_L \\ -\mathrm{i}\epsilon_L & 0 & -b_2 & 0 \\ 0 & -\mathrm{i}\epsilon_L & 0 & -b_1 \end{bmatrix} \tag{7}$$

where $b_1 = \mu_0(\frac{3}{2}g_1' + \frac{27}{8}g_2')B$, $b_2 = \mu_0(\frac{1}{2}g_1' + \frac{1}{8}g_2')B$ describe the linear Zeeman effect and $\epsilon_L = p_d E$ describes the linear Stark effect. Mixing of $u_{J=\frac{3}{2},\frac{3}{2}}$ with $u_{J=\frac{3}{2},-\frac{1}{2}}$ and $u_{J=\frac{3}{2},\frac{1}{2}}$ with $u_{J=\frac{3}{2},-\frac{3}{2}}$ makes each of transitions shown in figure 4(a) active in both circular polarizations, which is a reason for the decrease of γ_C with an increase of E.

A detailed discussion of a $\gamma_C(E)$ dependence resulting from the Hamiltonian (7) is given in [6], where conditions for observation of the Stark effect in acceptor δ-doped heterostructures are specified. In brief, it is shown that observation of the Stark effect is possible by magnetoluminescence polarization spectroscopy on heterostructures with the δ-layer placed at about 20 nm from the interface at temperatures of about 100 mK and magnetic fields below 1 T. Essential results are summarized in figure 5. For the range of n_s considered, the electric field at the position of the δ-layer at 30 nm from the interface is practically independent of n_s (figure 5(a)) and too weak to cause observable changes in γ_C (figure 5(b)). We thus conclude that the Stark effect in the heterostructure investigated is too small to lead to $\gamma_C(n_s)$ observed. The above estimation is based on the $L = 0$ model, but taking into account the $L = 2$ part of the envelope leads to considering higher-order effects, which does not change the above conclusion.

Let us discuss now the Pockels effect, i.e., the birefringence induced by the electric field. In the case considered of a crystal of the T_d symmetry and the electric field in the [001] direction, a difference in optical constants is induced for photon polarization parallel to the $[1\bar{1}0]$ and [110] directions. This leads to a linear polarization of optical transitions, with the degree of polarization defined as $\gamma_L = (I_{[110]} - I_{[1\bar{1}0]})/(I_{[110]} + I_{[1\bar{1}0]})$, where $I_{[110]}$ and $I_{[1\bar{1}0]}$ are intensities of light observed for a given polarization. A phenomenological description of the optical anisotropy [8] shows that γ_L and γ_C are related to each other: $\gamma_C \sim \sqrt{1-\gamma_L^2}$, which means that an increase of γ_L induced by the electric field correlates with a decrease of γ_C. This explains why, in principle, the Pockels effect can be responsible for the $\gamma_C(n_s)$ dependence observed.

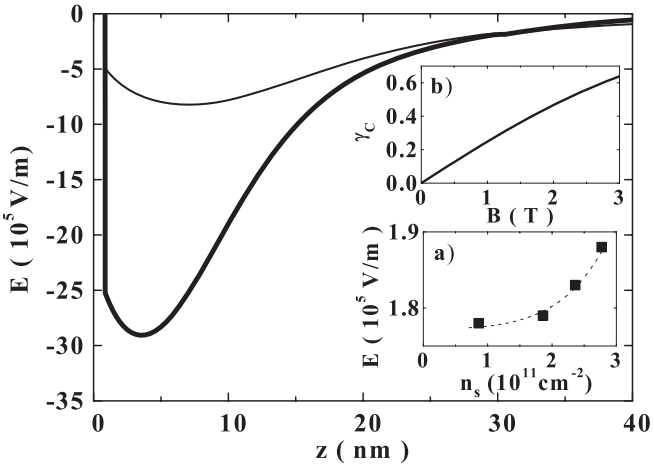

Figure 5. The heterostructure electric field for $n_s = 0.35 \times 10^{11}$ cm^{-2} (thin line) and 2.77×10^{11} cm^{-2} (thick line). (a) The electric field at $z_0 = 30$ nm as a function of the electron concentration n_s. The dashed line is a guide to the eyes. (b) The $\gamma_C(B)$ dependence calculated on the basis of energies and wavefunctions obtained by diagonalization of the Hamiltonian given by equation (7) at 1.6 K and for[4] $p_d = 1D$ ($1D = 3.3 \times 10^{-30}$ C m). γ_C for $E = 0$ and $E = 1.9 \times 10^5$ V m^{-1} cannot be distinguished in the scale of the figure.

An analysis of the Pockels effect carried out in connection with optical transitions in quantum wells [8–11] involves valence band holes and cannot be directly applied in the present case, because valence band holes do not participate in the optical transition analysed. Rössler and Kainz showed, however, that taking into account the **kp** coupling of bands, perturbation of the valence band by a Hamiltonian proportional to $\{J_x, J_y\}$ leads to a [110] versus [1$\bar{1}$0] anisotropy of the conduction band in the third order of perturbation [12]. Starting from a perturbation $H_a = GE(J_xJ_y + J_yJ_x)$, one gets the following effective perturbation of the conduction band:

$$H_c = G\frac{P^2}{E_0^2}\left\{\left(\frac{1}{3}+\frac{2}{3}\frac{E_0}{E_0+\Delta}\right)E(z)k_xk_yI_{2x2} + \mathrm{i}\left(\frac{1}{6}-\frac{E_0}{6(E_0+\Delta)}\right)[k_z, E(z)](k_x\sigma_x - k_y\sigma_y)\right\}, \tag{8}$$

where G is of the order of 10^{-9} eV cm V^{-1} $\sim 1D$ [13]. $I_{2\times2}$ is a two-dimensional unit matrix, k_i are components of the electron wavevector, and σ_i are Pauli spin matrices. $P = 10.493$ eV Å is the Kane matrix element of the optical transition, $E_0 = 1.52$ eV is the GaAs energy gap, and $\Delta = 0.341$ eV is the spin–orbit splitting in GaAs (numerical values are taken from table D.1 of [14]). The diagonal terms of H_c are of C_{2v} symmetry, and they describe the anisotropy of the conduction band resulting from the Pockels effect[5]. Since the perturbation Hamiltonian is of the same form as that of equation (6), the Pockels effect leads to selection rules as in the case of the Stark effect.

To estimate the upper limit of the Pockels effect, we take k equal to the Fermi vector for the highest concentration considered in calculations, 2.77×10^{11} cm^{-2}, and the maximal value

[4] Since the value of p_d for a Be acceptor in GaAs is apparently not known, we assumed in calculations $p_d = 1D$, which is of the order of dipole moments found by Köpf and Lassmann for several shallow acceptors in Si [7].

[5] The off-diagonal terms describe the spin splitting and are neglected in the present analysis since we consider an equal number of electrons with spin up and spin down. On the other hand, they are as small as the diagonal terms are, and can be neglected due to their negligible influence on electron wavefunctions.

of E for this n_s. Taking $k_x = k_y = k_F/\sqrt{2} = 9.7 \times 10^7$ m^{-1} and $E = 3 \times 10^6$ V m^{-1} (see figure 5) one finds the perturbation energy of each of the conduction band states to be of the order of 10^{-5} meV. This energy is far too small to indicate any observable changes in electron wavefunctions. This means that a [110] versus [1$\bar{1}$0] anisotropy of electron wavefunctions can be neglected[6]. Thus we have shown that the heterostructure electric field is too small to change γ_C in a noticeable way.

The above discussion allows us to conclude that the source of the $\gamma_C(n_s)$ dependence observed is the presence of the $L = 2$ part of the acceptor envelope wavefunction. According to the results presented in figure 3, to observe a decrease in γ_C of 1%, n_s should change by about 10^{11} cm^{-2}. This explains why a $\gamma_C(n_s)$ dependence was not observed in [1] which reports investigation on samples with n_s below 10^{11} cm^{-2}. Let us also note that the methodology of the present paper is just the opposite to that of [1]: we consider a 2DEG with defined (equal to zero) spin polarization and we analyse γ_C to study the properties of a Be acceptor. This approach allows us to show that an interband polarization spectroscopy in δ-doped heterostructures can be used to investigate the structure of the ground state of shallow acceptors.

The intensity of additional transitions allowed within the $L = 0, 2$ model is, in general, a few orders of magnitude smaller than of those allowed within the $L = 0$ model. Additional transitions appear because the electron wavefunction $\psi_n(z)$ is not constant within the volume spanned by the $L = 2$ part of the acceptor envelope. In the present analysis we neglected cubic corrections to the acceptor ground state [15]. Within the cubic model, the acceptor envelope is described by a series including spherical harmonics with all even L values. In such a case, any pair of electron and hole levels in figure 4 would be connected by a transition allowed in both circular polarizations. We expect, however, that transitions additional to these shown in figure 4(b) are negligible, since they result from higher-order perturbations to the $L = 0, 2$ model.

6. Summary and conclusions

Low-temperature polarized magnetoluminescence experiments on a high-quality GaAs/AlGaAs heterostructure with a Be acceptor δ-layer incorporated into the GaAs channel were carried out. A metallic gate prepared on the sample surface allowed us to tune the 2DEG concentration in the heterostructure. The degree of circular polarization of the luminescence originating from transitions between the 2DEG and photoexcited holes bound to Be acceptors was analysed. We observed that γ_C decreases with the increase of n_s. We discussed three mechanisms that can, in principle, explain the $\gamma_C(n_s)$ dependence observed: the presence of an $L = 2$ part of the acceptor envelope wavefunction, the Stark effect on a Be-localized hole, and an in-plane optical anisotropy induced by the heterostructure electric field (the Pockels effect). An analysis of the Stark and Pockels effects showed that they can be neglected in the heterostructure investigated. Calculations of $\gamma_C(n_s)$ taking into account the $L = 2$ part of the acceptor envelope allowed us to explain the $\gamma_C(n_s)$ dependence quantitatively. We thus show that interband polarization spectroscopy in acceptor δ-doped heterostructures allows one to investigate the ground state of shallow acceptors in bulk GaAs.

Acknowledgments

JŁ is thankful to M Grynberg, A Łusakowski and P Pfeffer for discussions.

[6] We are thankful to P Pfeffer for carrying out detailed calculations, based on the Hamiltonian (8), and also of the Rashba effect, confirming the negligible role of these perturbations in the heterostructure studied.

References

[1] Kukushkin I V and Timofeev V B 1996 *Adv. Phys.* **45** 147
[2] Filin A I, Dite A F, Kukushkin I V, Volkov O V and von Klitzing K 1992 *JETP Lett.* **56** 156
[3] Baldereschi A and Lipari N O 1973 *Phys. Rev.* B **8** 2697
[4] Bhattacharjee A and Rodriguez S 1972 *Phys. Rev.* B **6** 3836
[5] Bir G L, Butikov E I and Pikus G E 1963 *J. Phys. Chem. Solids* **24** 1467
[6] Łusakowski J, Sakowicz M, Friedland K J and Ploog K 2007 *Solid State Commun.* **142** 299
[7] Köpf A and Lassmann K 1992 *Phys. Rev. Lett.* **69** 1580
[8] Yakovlev D R, Platonov A V, Ivchenko E L, Kochereshko V P, Sas C, Ossau W, Hansen L, Waag A, Landwehr G and Molenkamp L W 2002 *Phys. Rev. Lett.* **88** 257401
[9] Kwok S H, Grahn H T, Ploog K and Merlin R 1992 *Phys. Rev. Lett.* **69** 973
[10] Platonov A V, Kochereshko V P, Ivchenko E L, Mikhailov G V, Yakovlev D R, Keim M, Ossau W, Waag A and Landwehr G 1999 *Phys. Rev. Lett.* **83** 3546
[11] Ivchenko E L, Toropov A A and Voisin P 1998 *Phys. Solid State* **40** 1748
[12] Rössler U and Kainz J 2002 *Solid State Commun.* **121** 313
[13] Ye X L, Chen Y H, Wang J Z, Wang Z G and Yang Z 2001 *Phys. Rev.* B **63** 115317
[14] Winkler R 2003 *Spin–Orbit Coupling Effects in Two-Dimensional Electron and Hole Systems* (*Springer Tracts in Modern Physics* vol 191) (Berlin: Springer)
[15] Baldereschi A and Lipari N O 1974 *Phys. Rev.* B **9** 1525